ADVANCED TECHNOLOGIES AND MATERIALS VOL. 49, NO.2 (2024), 43-47
DOI: 10.24867/ATM-2024-2-005

1. Received: 15 November 2024
2. Revised: 25 November 2024
3. Accepted: 02 December 2024

Advanced Technologies & Materials

http://journal-atm.org
ISSN: 2620-0325 (print), ISSN: 2620-147X (online)

Original article

Enhancing Directed Energy Deposited AL5356 Through in Situ Workpiece Vibrations

[a]Mirza Imširović, [a]Uroš Trdan, [a]Damjan Klobčar*, [a]Drago Bračun, [b]Aleš Nagode, [c]Laurent Berthe, [d]Matija Bušić, [e]Miodrag Milčić, [e]Dragan Milčić, [e]Nataša Zdravković, [f]Aleksija Đurić

[a]*Faculty of Mechanical Engineering, University of Ljubljana, Aškerčeva 6, 1000 Ljubljana, Slovenia*
[b]*Faculty of Natural Sciences, University of Ljubljana, Aškerčeva 12, 1000 Ljubljana, Slovenia*
[c]*PIMM, UMR8006 ENSAM, CNRS, CNAM, 151 bd de l'Hôpital, 75013 Paris, France*
[d]*Department of Mechanical Engineering, University North, University Center Varaždin, Jurja Križanića 31b, 42000, Varaždin, Croatia*
[e]*University of Niš Faculty of Mechanical Engineering, Aleksandra Medvedeva 14, 18000 Niš, Serbia*
[f]*University of East Sarajevo, Faculty of Mechanical Engineering, , Vuka Karadžića 30, 71123 Sarajevo, Bosnia and Herzegovina*

ABSTRACT

This study explores an innovative method to enhance Directed Energy Deposition (DED) of aluminum 5356 products by integrating an electromagnetic vibration system into the DED setup. The application of vibrations significantly improved surface quality, reducing surface waviness and increasing building efficiency by 14%, from 78.5% to 92.25%.Gas porosity was reduced from 1.5 ± 0.04% in as-built (AB) components to 0.34 ± 0.07% in vibration-assisted (VA) parts. Tensile tests showed a marked reduction in anisotropy, with the tensile strength deviation between the x and z directions decreasing to less than 0.4% for vibration-assisted samples, compared to 7.9% for as-built ones. Additionally, secondary phase analysis revealed a homogenization effect, with magnesium- and iron-rich precipitates displaying a finer dispersion (3.57 ± 3.42 µm²) compared to 11.28 ± 12.49 µm² in as-built parts. Overall, the findings highlight the potential of vibration-assisted DED to improve part properties, reduce defects, and advance the DED manufacturing process.

Key words: *directed energy deposition (DED), vibrations, residual stress, gas porosity, grain refinement.*

1. INTRODUCTION

Direct Energy Deposition (DED) is a promising 3D manufacturing technology for largescale metal components, offering deposition rates of 50-130 g/min. Based on established welding techniques such as Gas Metal Arc Welding (GMAW), Gas Tungsten Arc Welding (GTAW), and Plasma Arc Welding (PAW), DED can work with various materials, including stainless steels, titanium alloys, and aluminium alloys [1].

Aluminium alloys, particularly the 5xxx series, are highly regarded for their lightweight properties, high strength, corrosion resistance, and good weldability, making them ideal candidates for DED. The high thermal conductivity of aluminium also helps reduce manufacturing times, enhancing efficiency in producing parts for applications in aerospace, marine, and other industries [2]. Despite its advantages, DED faces challenges typical of layer-by-layer additive manufacturing. High heat input and rapid cooling can lead to uneven residual stresses, causing premature

* *Corresponding author's.e-mail: damjan.klobcar@fs.uni-lj.si*
Published by the University of Novi Sad, Faculty of Technical Sciences, Novi Sad, Serbia.

failure and distortion. Additional issues like gas porosity from contaminants can compromise structural integrity, while microstructural anisotropy impacts mechanical properties [3], [4]. To mitigate these defects, careful selection of process parameters such as gas flow rate and interpass temperature is essential, though post-processing treatments like heat annealing and surface modifications often remain necessary, adding time and cost [5].

Recent advancements in alternative mid-processing techniques, such as interlayer rolling and ultrasonic vibrations, show promise in addressing these issues. Ultrasonic vibrations, in particular, can significantly improve melt pool dynamics, reducing porosity and enhancing grain structure, though their stability over time presents challenges [6].

This study aims to evaluate the integration of subsonic in-situ vibrations during DED to improve microstructural homogeneity, alleviate residual stresses, reduce gas porosity, and enhance surface quality. Focusing on the Al 5356 alloy, known for its corrosion resistance and strength-to-weight ratio, this approach could enhance manufacturing efficiency while maintaining high product quality, contributing to more stable, energy-efficient, and cost-effective fabrication processes in various industrial applications.

2. METHOLOGY

The methodology (Fig.1) employed in this study involved fabricating metal walls using an ABB IRB 140 robotic arm with a MIG torch, utilizing the CMT+P metaltransfer mode Two wall configurations were employed, one using standard process and the other utilizing an integrated electromagnetic vibration system. The filler material (Table 1), ER5356, was used across both configurations, with specific process parameters detailed in Table 2. Monitoring was conducted using a Cavitar camera and thermocouples to ensure optimal conditions throughout the deposition process.

Table 1 - *Filler and substrate chemical composition (wt.%) [7]*

Element	Mg	Si	Fe	Cu	Mn	Zn	Ti	Cr	Al
Filler	5	0.06	0.12	0.08	0.12	0.007	0.12	0.09	bal.
Substrate	0.05	0.05	0.1	0.05	0.05	0.1	0.05	/	bal.

Table 2 - *Direct Energy Deposition process parameters*

Parameter	No. of layers [-]	Arc current [A]	Arc voltage [V]	Cooling time [s]	Travel speed [mm/s]	Wire feed speed [m/min]	Gas flow rate [l/min]
Value	40	49	14	45	10	2.5	12

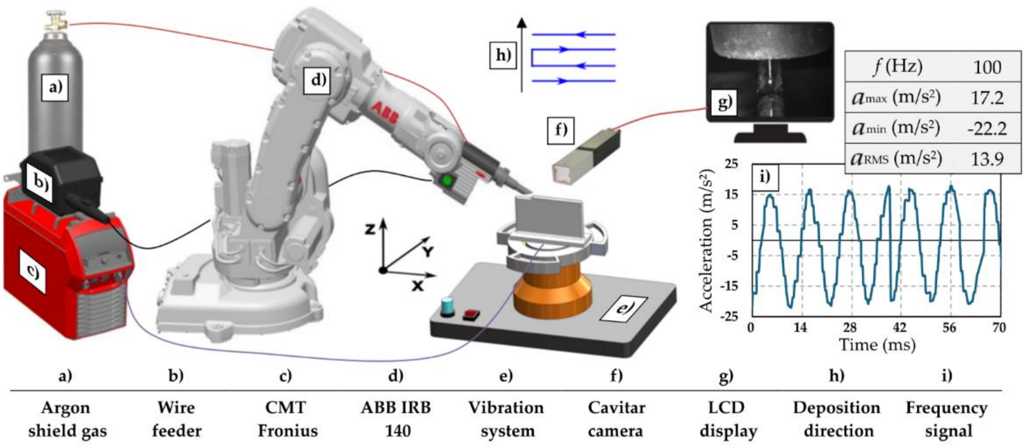

Fig. 1 *DED experimental setup with integrated electromagnetic vibration system*

Two wall configurations were employed, one using standard process and the other utilizing an integrated electromagnetic vibration system. The filler material (Table 1), ER5356, was used across both configurations, with specific process parameters detailed in Table 2. Monitoring was conducted using a Cavitar camera and thermocouples to ensure optimal conditions throughout the deposition process.

The chemical compositions of the filler wire and substrate were documented, with AF12 aluminium alloy serving as the substrate for this experiment.

2.1 *Sample preparation and microstructural analysis*

Samples for microstructure and porosity analysis were prepared by cutting the manufactured walls from cross-sectional areas. Samples were ground using SiC papers (#600, #1200, #2000) and polished for examination. The Thermo Scientific Quattro S SEM with EDS was used to observe element concentrations and precipitates. Python was employed for particle size/distribution analysis and magnesium segregation rates based on EDS mapping.

Precipitate isolation and element quantification were conducted using the Nearest Neighbor Index method.

2.2 Geometry and porosity analysis

The prepared samples were examined using a Keyence 6000 VHX digital-optical microscope at 50x magnification to analyze surface features. Porosity analysis was performed using ImageJ, following the process in Fig.2a.
The RGB channels were separated to select the highest contrast image and the threshold adjusted to capture porosity particles and gas porosity was calculated by dividing the sum of selected particles by the image area. Multiple measurements were used to optimize average porosity values for accurate quantification.
Geometrical properties were assessed using a Python-based image processing program as shown in Fig.2b.

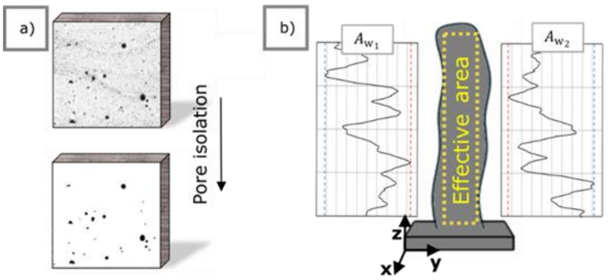

Fig. 2 *Porosity and geometry analysis: a) pore isolation via ImageJ, b) schematic waviness determinetion on both sides*

2.3 Tensile testing

For tensile testing, samples from both the x-direction and z-direction of the fabricated walls were cut with water jet and tested. The tests were performed using a 50 kN universal testing machine to evaluate the material's tensile properties, including ultimate tensile strength (UTS), yield strength, and elongation at break.
The results from the x and z orientations were compared to assess anisotropy in mechanical properties. The tensile test specimen used in this study had a length (L) of 40 mm, a gauge length (l_0) of 15 mm, and a gauge width (b_0) of 2.4 mm. The overall width (B) was 10 mm, with a fillet radius (R) of 5 mm.

3 Results and discussion

3.1 Geometry analysis

In Fig.3a, the deposited layer of AB sample shows significant waviness, as indicated by the red dashed lines. This waviness suggests inconsistent melt pool dynamics, resulting in uneven layer deposition.
Fig.3b illustrates the effect of vibration assistance. The melt pool exhibits a partial collapse, shown by the orange arrows, indicating more dynamic melt pool behavior. The vibrations help break up the surface tension of the melt pool, leading to better flow and redistribution of material. This agitation flattens the deposited layer, reducing surface waviness compared to the AB sample, resulting in a smoother, more consistent deposition.

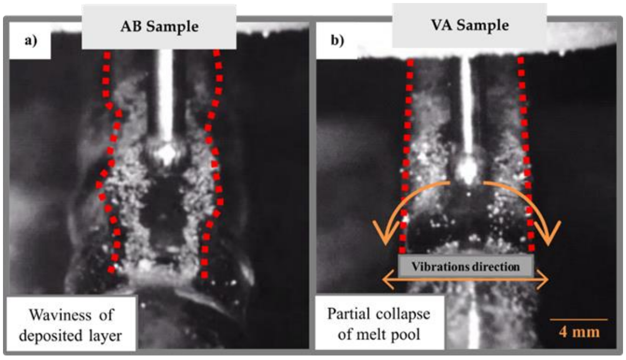

Fig. 3 *Cavitar images of meltpool: a) AB sample, b) VA sample*

Table 3 contains the waviness measurements and building efficiency factors for the AB and VA samples in the WAAM process. The AB sample exhibits higher maximum waviness (+420 µm and +370 µm) compared to the VA sample (+160 µm), indicating more distinct transitions between deposited layers due to inadequate melt pool stabilization. The reduced waviness in the VA sample, with a minimum of -90 µm, reflects smoother layer transitions attributed to vibration-assisted melt pool agitation, which enhances material flow. Consequently, the building efficiency improves significantly from 78.5% for the AB sample to 92.25% for the VA sample, demonstrating the effectiveness of vibrations in promoting superior surface quality and operational efficiency in additive manufacturing processes.

3.2 Gas porosity analysis

In the AB sample porosity decreases as the interpass temperature increases from the bottom to the top of manufactured product (Table 4). At the bottom significant porosity and larger merged pores are visible, indicating poor degassing at low temperatures, due to high cooling rate. As the interpass temperature increases toward the middle and top, the porosity reduces slightly, but remains substantial, with large pores still present due to insufficient melt pool agitation and gas entrapment during deposition.
In contrast, the VA sample shows a significant reduction in porosity at all cross-sectional levels. Vibration-assisted deposition promotes better melt pool agitation, enhancing degassing and preventing pore formation.
The combination of vibrations and increased temperature promotes more efficient gas escape from the melt pool, leading to a more homogenous and less porous structure throughout the part. The comparison clearly highlights the benefits of vibration assistance, where the continuous agitation of the melt pool, combined with rising interpass temperatures, effectively enhances degassing, reduces porosity, and leads to improved material quality.

3.3 EDS analysis

Fig.4 compares magnesium and iron segregation in AB and VA samples. In Fig.4a, the AB sample shows pronounced magnesium segregation, with a segregation rate (SR) of 0.41% and larger peak areas (9.05 ± 9.53 μm²). The nearest neighbor index (NNI) is low (0.089), indicating clustered magnesium distribution.
Fig.4b shows the VA sample, where magnesium segregation is less prominent, with an SR of 0.23%, smaller peak areas (3.44 ± 3.52 μm²), and a higher NNI (0.225), reflecting a more dispersed pattern.

Table 3: *Waviness measurements and building efficiency results.*

Sample	Profile	Max Waviness (μm)	Min Waviness (μm)	RMS Waviness (μm)	Building efficiency (%)
AB Sample	W1	+420	-430	420	78.5
AB Sample	W2	+370	-430	370	
VA Sample	W1	+160	-90	160	92.25
VA Sample	W2	+150	-120	150	

Table 4: *Porosity distribution and interpass temperature effects in WAAM-assisted aluminum deposition for AB and VA samples*

Sample Type	Location	Temperature (°C)	Porosity (%)	Average Pore Area (μm²)
AB Sample	Bottom	45	1.82	2771.8 ± 4410.2
	Middle	135	1.33	1937.0 ± 2820.0
	Top	185	1.35	1931.7 ± 2560.7
VA Sample	Bottom	50	0.42	1292.7 ± 2554.3
	Middle	130	0.34	833.66 ± 1359.8
	Top	170	0.27	856.9 ± 1082.0

Fig.4c displays iron segregation in the AB sample, where the SR is higher at 0.59%, with larger peak areas (13.38 ± 12.49 μm²) and an NNI of 0.110, indicating significant clustering.
In Fig.4d, iron segregation in the VA sample is less pronounced, with an SR of 0.25%, smaller peak areas (3.87 ± 3.42 μm²), and an NNI of 0.331, indicating a more uniform distribution. These results highlight the substantial effect on homogenization of melt pool induced by vibrations.

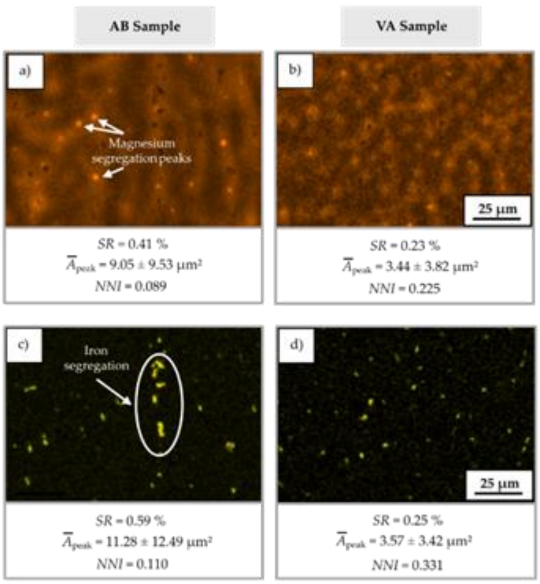

Fig.4 *Elemental segregation: a) magnesium in AB sample, b) magnesium in VA sample, c) iron in AB sample, d) iron in VA sample*

3.4 Tensile testing results

Fig.5a presents the stress-strain curves for AB and VA specimens, measured along the x and z directions. The black and yellow curves represent AB samples, while the green and blue curves show VA samples.

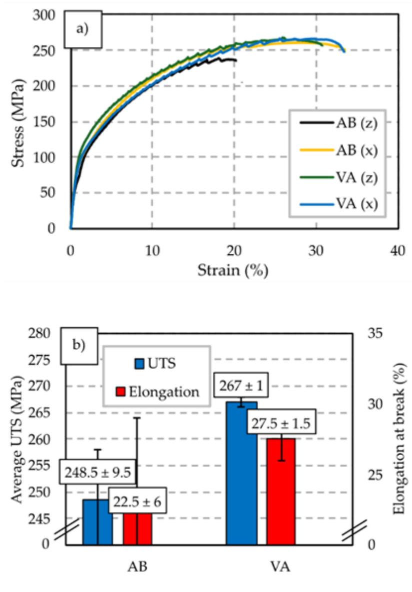

Fig.4 *a) Tensile testing results, b) average UTS and elongation at break.*

A notable improvement in tensile strength is observed for VA samples in the z-direction, with a 12.1% increase compared to the AB sample (268 MPa vs. 239 MPa). This indicates that the VA samples exhibit a more isotropic mechanical state, with only a 0.4% difference between the x and z directions, whereas the AB samples show a larger 7.9% difference in UTS between these directions.

Fig.5b summarizes the average ultimate tensile strength (UTS) and elongation at break for both AB and VA samples. The VA samples show higher UTS at 267 ± 1 MPa, compared to 248.5 ± 9.5 MPa for AB samples. Additionally, the VA samples exhibit greater ductility, with an elongation at break of 32.5 ± 1.5%, versus 28 ± 6% for AB samples. The improved mechanical properties in VA samples are attributed to a 25% reduction in grain size, decreased gas porosity, and a significant relaxation of residual stress in the z-direction due to in-situ vibrations, which contributes to their more uniform and isotropic behavior.

4 CONCLUSION

The integration of subsonic in-situ vibrations during the Direct Energy Deposition of Al 5356 alloy demonstrates significant advantages over conventional methods. The study's findings reveal the following key conclusions:

- The application of vibrations resulted in improved melt pool behavior, reducing waviness and promoting smoother layer transitions. This enhancement led to a significant increase in building efficiency from 78.5% for standard samples to 92.25% for vibration-assisted samples.
- Vibration assistance effectively mitigated gas porosity. (1.5 ± 0.04% vs. 0.34 ± 0.07%). This reduction was attributed to better melt pool agitation, which facilitated more efficient gas escape and a more homogeneous structure.
- Study observed a marked decrease in magnesium and iron segregation in the vibration-assisted samples. This suggests that vibrations contribute to a more uniform elemental distribution, leading to improved material properties.
- The tensile testing revealed a notable enhancement in ultimate tensile strength and ductility for vibration-assisted samples, with UTS increasing by 12.1% in the z-direction. This improvement is linked to reduced grain size, decreased gas porosity, and alleviated residual stresses.

The successful integration of vibrations in DED processes not only addresses common defects associated with additive manufacturing but also contributes to the production of high-quality components with desirable mechanical properties. This approach presents a viable solution for industries requiring efficient, reliable, and high-performance metal fabrication.

ACKNOWLEDGEMENT

This research was financially supported by the Slovenian Research Agency under grant number P2-0270 and bilateral projects Weave N2-0328 and BI-BA/24-25-034. The project proposal was also partly supported by EU ERASMUS+ Strategic Partnership Key Action 2, numbers 2021-1-RO01-KA220-VET-000028028 (DIGIGREEN) and 2023-1-RO01-KA220-HED-000158031 (ANGIE).

REFERENCES

[1] Singh, S. R., Khanna, P. (2021) Wire arc additive manufacturing (WAAM): A new process to shape engineering materials, in Materials Today: Proceedings, Elsevier Ltd, pp. 118–128. doi: 10.1016/j.matpr.2020.08.030.

[2] Trdan U., Grum, J. (2012) Evaluation of corrosion resistance of AA6082-T651 aluminium alloy after laser shock peening by means of cyclic polarisation and ElS methods. *Corros Sci*, 59, 324–333, doi: 10.1016/j.corsci.2012.03.019.

[3] Wang, J., Zhu, K., Zhang, W., Zhu, X., Lu, X. (2023) Microstructural and defect evolution during WAAM resulting in mechanical property differences for AA5356 component. *Journal of Materials Research and Technology*, 22, 982–996, doi: 10.1016/j.jmrt.2022.11.116.

[4] Wu B. et al. (2018) A review of the wire arc additive manufacturing of metals: properties, defects and quality improvement, Elsevier Ltd. doi: 10.1016/j.jmapro.2018.08.001.

[5] Pan, Z., Ding, D., Wu, B., Cuiuri, D., Li, H., Norrish, J. (2018) Arc Welding Processes for Additive Manufacturing: A Review. Transactions on Intelligent Welding Manufacturing, pp. 3–24. doi: 10.1007/978-981-10-5355-9_1.

[6] Tan, C. et al. (2023) Review on field assisted metal additive manufacturing. *Int J Mach Tools Manuf*, 189, p. 104032, doi: 10.1016/J.IJMACHTOOLS.2023.104032.

[7] 5356 Aluminium Wire https://www.digitalweld.co.nz/product/bohler-union-almg5/. Accessed: Nov. 09, 2023.

NOTE

This paper is based on the paper presented at 7th International scientific conference ”Conference on Mechanical Engineering Technologies and Applications” COMETa 2024, 14th – 16th November, 2024, East Sarajevo, B&H.